의학박사 학위논문

CKD-5, a Novel Pan-histone Deacetylase Inhibitor, Synergistically Enhances the Efficacy of Sorafenib for Hepatocellular Carcinoma

간세포암에서 CKD-5와 소라페닙 병용요법의 상승적 항암효과

2021년 2월

서울대학교 대학원
의학과 내과학
장 영

간세포암에서 CKD-5와 소라페닙 병용요법의 상승적 항암효과

CKD-5, a Novel Pan-histone Deacetylase Inhibitor, Synergistically Enhances the Efficacy of Sorafenib for Hepatocellular Carcinoma

지도교수 **윤 정 환**

이 논문을 의학박사 학위논문으로 제출함

2020년 10월

서울대학교 대학원

의학과 내과학

장 영

장영의 의학박사 학위논문을 인준함

2021년 1월

위 원 장 (인)

부위원장 (인)

위 원 (인)

위 원 (인)

위 원 (인)

CKD-5, a Novel Pan-histone Deacetylase Inhibitor, Synergistically Enhances the Efficacy of Sorafenib for Hepatocellular Carcinoma

by

Young Chang, M.D.

A Thesis Submitted to the Department of Internal Medicine
in Partial Fulfillment of the Requirements
for the Degree of Doctor of Philosophy in Medicine
at the Seoul National University College of Medicine

January, 2021

Approved by thesis committee:

Professor Yong Tae Kim Chairman
Professor Jung-Hwan Yoon Vice Chairman
Professor Kyung Suk Suh
Professor Kwang-Woong LEE
Professor Si Hyun Bae

Abstract

CKD-5, a Novel Pan-histone Deacetylase Inhibitor, Synergistically Enhances the Efficacy of Sorafenib for Hepatocellular Carcinoma

Young Chang

Department of Internal Medicine

Seoul National University College of Medicine

Background: Histone deacetylase inhibitors (HDACIs) have distinctive epigenetic targets involved in hepatocarcinogenesis and chemoresistance. A recent phase I/II study reported the possibility of HDACI as a chemosensitizer in sorafenib-resistant patients. In this study, we evaluated whether CKD-5, a novel pan-HDACI, can potentiate the efficacy of sorafenib.

Methods: The anticancer effect of CKD-5 with and without sorafenib was evaluated in vitro using an MTS assay with human HCC cells (SNU-3058 and SNU-761) under both normoxic and hypoxic conditions. Microarray analysis was performed to investigate the mechanism of cell death, which was also evaluated by small interfering RNA (siRNA) transfection and subsequent immunoblot assays. In vivo experiments were conducted using two different murine HCC models. C3H mice implanted with MH134 cells and C57BL/6 mice implanted with RIL-175 cells were

treated with weekly CKD-5 with and without sorafenib for 2 weeks.

Results: CKD-5 treatment significantly suppressed human HCC cell growth in both normoxic and hypoxic conditions. Microarray analysis and real-time PCR showed that CKD-5 treatment significantly increased peripherin expression in HCC cells and that downregulation of peripherin by siRNA decreased CKD-5-induced apoptosis. The combination of CKD-5 and sorafenib decreased cell viability more effectively than sorafenib or CKD-5 monotherapy in human and murine HCC cells. The effectiveness of the combination therapy was consistently demonstrated in the animal models. Histological and biochemical analyses demonstrated good tolerance of CKD-5 plus sorafenib *in vivo*.

Conclusions: CKD-5 may enhance sorafenib efficacy through epigenetic regulation. The combination of CKD-5 and sorafenib might be a novel therapeutic option for the treatment of HCC.

Key words: Histone deacetylase inhibitor; CKD-5; Hepatocellular carcinoma; Sorafenib

Student Number: 2017-39124

List of Figures

Contents

Introduction

Hepatocellular carcinoma (HCC) is the most common primary malignancy of the liver. Liver cancer is predicted to be the fifth most commonly diagnosed cancer and the second leading cause of cancer mortality worldwide in 2018.[1] Owing to its global disease burden and poor prognosis, HCC remains a major global health problem. There are various effective treatments for early to intermediate stage HCC such as surgical resection, radiofrequency ablation, trans-arterial chemoembolization, and transplantation. In contrast, patients with advanced HCC have very poor prognoses and limited effective treatments. Sorafenib, a multi-kinase inhibitor, was established as a standard treatment for advanced HCC patients based on the results of the SHARP (Sorafenib HCC Assessment Randomized Protocol) trials.[2] In clinical practice, however, there have been limitations in treating advanced HCC patients with sorafenib because it has demonstrated limited survival benefits with low tumor response rates, suggesting the existence of sorafenib-resistance.[3] To overcome these limitations of sorafenib, combination therapies with various treatment modalities such as locoregional treatment [4-6], conventional chemotherapy [7-9], and novel targeted agents [10-12] have been tried.

Histone deacetylase inhibitors (HDACIs) have been extensively studied and are considered promising anticancer agents based on preclinical and clinical trials.[13, 14] Many clinical trials have proved the efficacy of HDACIs in hematologic malignancies, including various kinds of lymphoma, and in thymoma and

melanoma.[14] Based on the positive results of these clinical trials, the US FDA firstly approved panobinostat, a non-selective HDACI, for treatment of progressive or relapsed T cell lymphoma in the United States in 2006; it was approved in Korea in 2012. Also, HDACI efficacy against advanced HCC has been suggested in a preclinical study.[15]

CKD-5 is a novel hydroxamic acid-based pan-HDACI under investigation for the treatment of various tumor types. HDAC class I–II are major target of CKD-5[16], of which CKD-5 demonstrated potent inhibitory activity against human HDACs 1, 2, 3, and 8 (class I HDAC).[17] In preclinical *in vitro* and *in vivo* studies, CKD-5 has demonstrated strong anti-tumor effects against multiple myeloma and cutaneous T-cell lymphoma.[18, 19] CKD-5 has also shown considerable cytotoxicity in multiple solid tumor cell lines and xenograft mouse models of colon, prostate, and lung cancer.[20] A phase I study of CKD-5 recently reported promising results with minimal side effects and modest anti-tumor efficacy in patients with lymphoma or multiple myeloma refractory to standard therapy.[17] In this study, we demonstrated that CKD-5 has consistent anti-tumor effects in various HCC cell lines and xenograft mice models, which is further potentiated when combined with sorafenib. This preclinical study establishes a rationale for clinical studies of HDACI therapy for HCC.

Materials and methods

Cell lines and cell culture

Five HCC cell lines were used: Huh-7[21], a well differentiated HCC cell line; SNU-761[22], a poorly differentiated HCC cell line; SNU-3058[23], a hypovascular HCC cell line provided by the Korea Cell Line Bank; MH-134[24] and RIL-175[25] (provided by Professor T. Greten, NIH) murine HCC cell lines. Cells were grown in RPMI 1640 supplemented with 10% fetal bovine serum (FBS), 100,000 U/L penicillin and 100 mg/L streptomycin with or without 100 mM insulin.[26] In all experiments, cells were serum-starved overnight before the experiments to avoid the effect of serum-induced signaling. Cells were incubated under either standard normoxic (20% O_2 and 5% CO_2 at 37 °C) or hypoxic (1% O_2, 5% CO_2, and 94% N_2 at 37°C) conditions. As hypoxia induced by the rapid-growing nature of HCC, plays a critical role in HCC malignance and treatment failure, we performed the experiments in both normoxic and hypoxic conditions.[27]

Reagents and animals

CKD-5, a novel HDACI, was provided by Chong Kun Dang Pharmaceutical Corp. (Seoul, Korea). Panobinostat was purchased from Novartis Pharmaceuticals (East Hanover, NJ, USA). Sorafenib was purchased from LC Laboratories (Woburn, MA, USA). C3H mice and C57BL/6 mice were purchased from Orient Bio Inc. (Seongnam, Korea) for *in vivo* experiments.

Cell proliferation analysis (MTS assay)

Cell proliferation was measured on the basis of cellular conversion of the colorimetric reagent 3,4-(5-dimethylthiazol-2-yl)-5-(3-carboxymethoxyphenyl)-2-(4-sulfo-phenyl)-2H-tetrazolium salt (MTS) into soluble formazan by dehydrogenase enzyme found in metabolically proliferating cells with the Cell Titer 96 Aqueous One Solution cell proliferation assay (Promega, Madison, WI).[28] Following each treatment, 20 μL of dye solution was added into each well in 96-well plate and incubated for 2 hours. The absorbance was recorded at a wavelength of 490 nm using an enzyme-linked immunosorbent assay plate reader (Molecular Devices, Sunnyvale, CA, USA).

Complementary deoxyribonucleic acid (cDNA) microarray analysis

To compare relative gene expression profiles in human HCC cells after HDACI treatment, total ribonucleic acids (RNAs) from Huh-7 cells treated with HDACI (M171) or control reagent were extracted and purified. Microarray analysis was performed according to the Macrogen Rat Bead Chip technical manual (Macrogen, Seoul, Korea) using an Illumina RatRef-12 Expression Bead Chip (Illumina, Inc., San Diego, CA, USA).[28] Biotinylated cRNAs were prepared from 0.55 μg quantities of total RNA using the Illumina Total Prep RNA Amplification Kit (Ambion, Austin, TX, USA). After fragmentation, cRNAs were hybridized to the Illumina RatRef-12 Expression Bead Chip in 0.75 μg quantities using protocols provided by the

manufacturer. Arrays were scanned using the Illumina Bead Array Reader Confocal Scanner. Array data export processing and analysis were performed using Illumina Bead Studio v3.1.3 (Gene Expression Module v3.3.8).

Real-time polymerase chain reaction (PCR) analysis

Total RNA was extracted using Trizol Reagent (Invitrogen, Carlsbad, CA, USA). cDNA templates were synthesized using oligo-dT random primers and Moloney murine leukemia virus reverse transcriptase. After the reverse transcription reaction, the cDNA template was amplified by PCR using Taq polymerase (Invitrogen).[29] Peripherin and glutathione peroxidase 4 (GPX4) were quantitated by real-time PCR (LightCycler; Roche Molecular Biochemicals, Mannheim, Germany) using SYBR green as the fluorophore (Molecular Probes, Eugene, OR, USA). After electrophoresis in 1% agarose gel, the portion of gel containing the expected peripherin PCR product was excised, and the product was eluted into Tris-HCl using a DNA elution kit (Qiagen, Valencia, CA, USA). Primers for peripherin were AGCTACTGGAA GGGGAGGAG (forward) and CGGGTCTCAATTGTCCTGAT (reverse) [30, 31], and primers for GPX4 were TAAGAACGGCTGCGTGGTGAAG (forward) and AGAGATAGCACGGCAGGTCCTT (reverse).[32] Glyceraldehyde-3-phosphate dehydrogenase (GAPDH) gene expression was used as a control. Peripherin mRNA expression levels were calculated as the relative intensity of the PCR product bands compared with those of the GAPDH gene using the $2^{-\Delta\Delta Ct}$ method. All PCR experiments were performed in triplicate.

Small interfering RNA (siRNA) transfection

Cells were seeded in a 6-well culture plate (2 x 10^5 cells/well) in 2 mL antibiotic-free medium supplemented with 10% FBS. At 60%–80% confluence, the cells were transfected with siRNA using the siRNA Transfection Reagent (Santa Cruz Biotechnology Inc., Santa Cruz, CA, USA) according to the manufacturer's instructions. The cells were treated with siRNA for 6 hours at 37 °C and growth medium containing 20% FBS and antibiotics was added. After 18 hours, the medium was replaced with fresh medium containing 10% FBS and antibiotics, and 24 hours after transfection, the cells were used in the subsequent experiments.[28]

Immunoblot analysis

For the immunoblot analysis, 20 nM CKD-5 was treated 24 hours before, followed by treatment with 2 M sorafenib. Cells were lysed on ice for 20 minutes using lysis buffer (50 mM Tris-HCl, pH 7.4; 1% Nonidet P-40, 0.25% sodium deoxycholate; 150 mM NaCl; 1 mmol/L EDTA; 1 mM phenylmethylsulfonyl-fluoride; 1 mM Na3VO4; 1 mM NaF; and 1 mg/mL each of aprotinin, pepstatin, and leupeptin) and centrifuged at 14,000×*g* for 10 minutes at 4 °C. 50 g and 30 g of protein from SNU761 and SNU3058 cells, respectively, were loaded on a 12.5% SDS-PAGE gel. Samples were transferred to nitrocellulose membranes, blotted with appropriate primary antibodies at a dilution of 1:1000, and treated with peroxidase-conjugated secondary antibodies (Biosource International, Camarillo,

CA, USA). Bound antibodies were visualized using chemiluminescent substrate (ECL; Amersham, Arlington Heights, IL, USA) and exposed to Kodak X-OMAT film (Kodak, New Haven, CT, USA).[28] Primary antibodies included rabbit anti-caspase 9 and 7 (cleaved) (Cell Signaling Technology, Danvers, MA, USA), anti-heat shock protein 90 (HSP90), anti-P21 (both from Santa Cruz Biotechnology Inc., Santa Cruz, CA, USA), anti-GPX4, and anti-acetylated H3 (both from Abcam, Cambridge, UK). A goat anti-actin antibody was also used (Santa Cruz Biotechnology Inc., Santa Cruz, CA, USA).

In vivo subcutaneous xenograft mouse models

MH-134 cells (2.5 x 10^6/mL in 100 μL of RPMI-1640) were injected subcutaneously into the flank of 6-week-old C3H mice (n = 64).[33] Randomization into 8 groups with 8 mice each group was performed when the implanted MH-134 tumor bud reached a volume of 0.2 cm^3 in more than 60% of mice: control, low dose of CKD-5 (40 mg/kg), high dose of CKD-5 (60 mg/kg), panobinostat (10 mg/kg), sorafenib (30 mg/kg), panobinostat (10 mg/kg) + sorafenib (30 mg/kg), low dose of CKD-5 (40 mg/kg) + sorafenib (30 mg/kg), high dose of CKD-5 (60 mg/kg) + sorafenib (30 mg/kg). CKD-5 was injected intraperitoneally once a week (D0, D7) using a solution of 0.9% saline. Panobinostat was injected intraperitoneally 3 times a week (D0, D2, D4, D7, D9, and D11) using a solution of 0.9% saline with 10% ethanol and 10% Cremophor (Sigma, St. Louis, MO) as vehicle. Sorafenib was administered per gavage once daily (D0 to D13) using 0.5% carboxy-methylcellulose sodium as

vehicle. Animals were euthanized on day 14 to acquire tumor, liver, spleen, and blood samples for analysis. Euthanasia was performed by introducing 100% carbon dioxide gas in the chamber with a fill rate of 10% to 30% of the chamber volume per minute.

Repeated experiments were performed using the same mouse model with increased numbers of individuals in each group. A total of 35 C3H mice implanted with MH-134 HCC cells were assigned to 4 groups: control, CKD-5 (60 mg/kg), sorafenib (30 mg/kg), and CKD-5 (60 mg/kg) plus sorafenib (30 mg/kg). After randomization into 4 groups, experiments were conducted using the same protocol as in the previous experiments. To validate the results obtained with the MH-134/C3H mouse model, another xenograft mouse model was established. RIL-175 cells (2.5 x 10^6/mL in 100 μL of RPMI-1640) were injected into C57BL/6 mice [34], and experiments using the same protocol were performed.

Tumor volumes were measured using a Vernier caliper and calculated as a standard formula: $\pi/6$ x (length) x (width) ^{2}.[35] Pathologic analysis was performed using an Aperio image analyzer (Aperio Technologies, Inc., Vista, CA, USA). Staining positivity was defined as strong positive and positive results on Aperio image analysis.

Statistical analysis

All the experimental results were obtained from at least 3 independent *in vitro* experiments and at least 8 mice *in vivo* experiments and presented as the mean ±

standard deviation. For comparisons between groups, data were analyzed by student *t*-test, Mann-Whitney *U* test or one-way ANOVA. Before conducting Student's t-test, the normal distribution of variables was verified using Shapiro-Wilk test; Levene's test was performed to assess the homogeneity of variables between groups. Bliss independent analysis was conducted to confirm the synergistic anticancer efficacy of combination treatment.[36] For all tests, $P < 0.05$ was regarded as statistically significant. Statistical analyses were performed using PASW version 23.0 (IMB, Chicago, IL, USA).

Ethics statement

We carried out this study in strict accordance with the recommendations in the Guide for the Care and Use of Laboratory Animals of the National Institutes of Health. The *in vivo* study protocol was approved by the Institutional Animal Care and Use Committee (IACUC No. 18-0077-S1A0, 17-0060-C1A0) of Seoul National University Hospital.

Results

CKD-5 affected cell viability and apoptosis in HCC cell lines

CKD-5 treatment decreased SNU-761 and SNU-3085 cell proliferation in both normoxic and hypoxic conditions in a dose-dependent manner after 24-hour incubation (Figure 1A), and the anti-tumor effect was further enhanced after 48-hour incubation (Figure 1B). Also, CKD-5 enhanced apoptosis of HCC cells compared to controls, represented by increased expression of caspase-7 and -9 cleavages (Figure 2B). The cytotoxic efficacy of CKD-5 was further compared with that of panobinostat, a previously approved HDAC inhibitor, using SNU-761 cells. Both panobinostat and CKD-5 treatments reduced cell proliferation, and the cytotoxic efficacy was more potent when treated with CKD-5 than with panobinostat, especially in combination with sorafenib (Figure 3).

CKD-5 overexpressed peripherin in HCC cells, mediating CKD-5-induced HCC apoptosis

We sought to identify molecules that had altered expression after HDACI treatment of HCC cells to explain the mechanism of the CKD-5 anti-tumor effect. cDNA microarray analysis (Table 1 and Figure 4) showed significant peripherin overexpression after HDACI treatment compared to levels in controls with a 14.13-fold change. When SNU-761 and SNU-3058 cells were exposed to CKD-5, peripherin mRNA expression was significantly increased in both cell lines (Figure

2A).

To demonstrate the effect of CKD-5-induced peripherin overexpression in HCC cells, we transfected SNU-761 and SNU-3058 cells with control or peripherin siRNA and cultured the cells with CKD-5 for 24 hours. CKD-5-induced cleaved caspase-7 and -9 expression was downregulated by peripherin knockdown with siRNA (Figure 2B), indicating that CKD-5 induces HCC cell apoptosis via peripherin overexpression. We examined the expression of P21 and acetylated-HSP90, known to be involved in anti-tumor mechanisms of HDACI, by western blot after CKD-5 treatment. Neither acetylation of HSP90 nor p21 expression was altered after CKD-5 treatment (Figure 2C), suggesting that HSP90 and p21 are not involved in the anti-tumor mechanism of CKD-5.

CKD-5 and sorafenib synergistically inhibited HCC proliferation

The cytotoxicity of co-treatment with CKD-5 and sorafenib was evaluated in SNU-761, SNU-3085, MH-134, and RIL-175 cells. HCC cells were treated with 0–20 nM of CKD-5 and 0–4 μM of sorafenib, followed by MTS assay. Monotherapy with CKD-5 or sorafenib reduced the viability of HCC cells in a dose-dependent manner, and co-treatment with CKD-5 and sorafenib inhibited HCC cell proliferation significantly more than either sorafenib or CKD-5 monotherapy in all four HCC cell lines (Figure 5). The synergistic anticancer efficacy of the combination therapy with CKD-5 and sorafenib was demonstrated by an excess over Bliss score > 0 in all the investigated HCC cell lines (Table 2).

The combination therapy of CKD-5 and sorafenib induced more apoptosis in HCC cells than either CKD-5 or sorafenib monotherapy, showing highly expressed cleaved caspase-7 and -9 after CKD-5 and sorafenib combination treatment (Figure 6A). Histone acetylation levels increased with CKD-5 and sorafenib monotherapy, and the acetylation level was further increased by the combination treatment with CKD-5 and sorafenib (Figure 6B). Besides, the protein and mRNA expression of GPX4 was reduced by sorafenib treatment, suggesting that sorafenib induced ferroptosis in HCC cells. The effect was more significant in the combination treatment with sorafenib and CKD-5, suggesting that the induction of ferroptosis by sorafenib was further enhanced by CKD-5 combination (Figure 6B and 6C).

CKD-5 and sorafenib synergistically reduced tumor volume in xenograft mouse models

First, 64 C3H mice implanted with MH-134 HCC cells were divided into 8 groups (control, low-dose CKD-5, high-dose CKD-5, panobinostat, sorafenib, panobinostat plus sorafenib, low-dose CKD-5 plus sorafenib, and high-dose CKD-5 plus sorafenib) and treated with each drug or drug combination accordingly. After two weeks of treatment, all the treatment groups exhibited significantly more tumor volume reduction compared with the control group (all $P < 0.001$, Figure 7). In comparison with the sorafenib group, the CKD-5 groups and the CKD-5 plus sorafenib groups showed significantly decreased tumor volumes (all $P < 0.001$); in contrast, the panobinostat group and the panobinostat plus sorafenib group did not show

decreased tumor volumes (both $P = 1.000$).

Based on these results, repeated experiments were performed using the same mouse model with increased numbers in each group to evaluate the synergistic effect of combined CKD-5 and sorafenib. A total of 35 C3H mice implanted with MH-134 HCC cells were assigned to the following 4 groups: control, CKD-5 (60 mg/kg), sorafenib (30 mg/kg), and CKD-5 (60 mg/kg) plus sorafenib (30 mg/kg). After two weeks of treatment with each regimen, all the treatment groups showed significantly more tumor volume reduction than the control group (all $P < 0.001$). Additionally, the combination of CKD-5 and sorafenib resulted in significantly less tumor volume than either sorafenib ($P < 0.001$) or CKD-5 ($P = 0.001$) alone (Figure 8).

In a validation model of C57BL/6 mice implanted with RIL-175 HCC cells, CKD-5 combined with sorafenib significantly inhibited tumor growth more than either sorafenib or CKD-5 (both $P < 0.001$) monotherapy (Figure 9).

CKD-5 and sorafenib additively induced apoptosis and reduced vessel density in HCC xenografts

To further evaluate apoptosis and angiogenesis *in vivo*, terminal deoxynucleotidyl transferase dUTP nick end labeling (TUNEL) immunohistochemistry and hematoxylin and eosin (H&E) staining were performed. TUNEL staining revealed a marked increase of apoptotic cells in the tumor tissue of combination treated mice compared to sorafenib or CKD-5 treated mice (Figure 10) Additionally, the CKD-5 treated mice had decreased microvessel density compared to controls, which was

enhanced by combination with sorafenib, resulting in lower vessel density than in the control and sorafenib-treated mice (Figure 10).

Combination therapy with CKD-5 and sorafenib was well-tolerated without evidence of renal and hepatic toxicity

The levels of creatinine, alanine transaminase (ALT), and aspartate transaminase (AST) were examined to assess renal and hepatic toxicity of the combination therapy with CKD-5 and sorafenib. The combination treatment group showed significantly lower levels of creatinine and ALT, and the CKD-5 group showed significantly lower levels of ALT and AST, than the control group (Table 3). There were no significant differences in body weight between the treatment groups. These biochemical results demonstrate that there was no renal or hepatotoxicity in the combination therapy group.

Additionally, liver and spleen tissues of sacrificed mice were extracted, and the degree of apoptosis was assessed in both organs by TUNEL and H&E staining to identify toxicities of each treatment. Little apoptosis of the liver and spleen tissues was detected in all treatment groups (Figure 11).

Figures

A

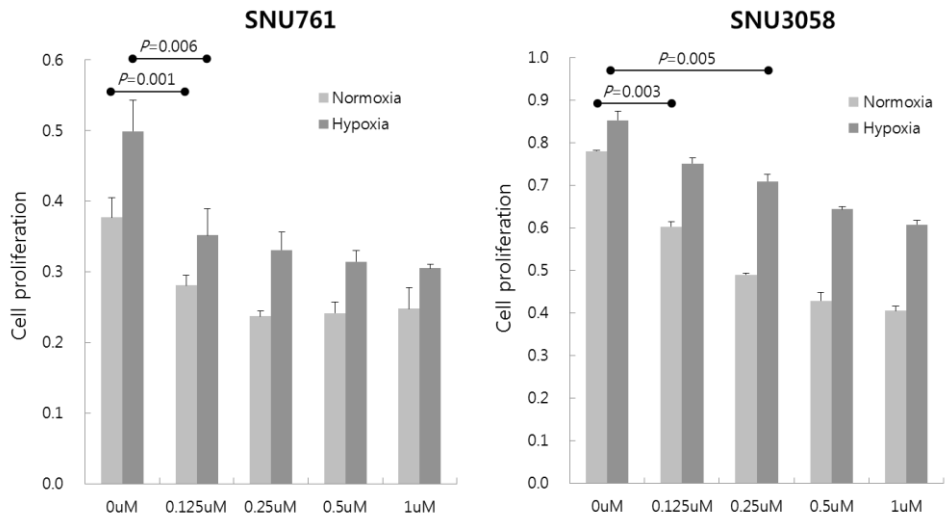

B

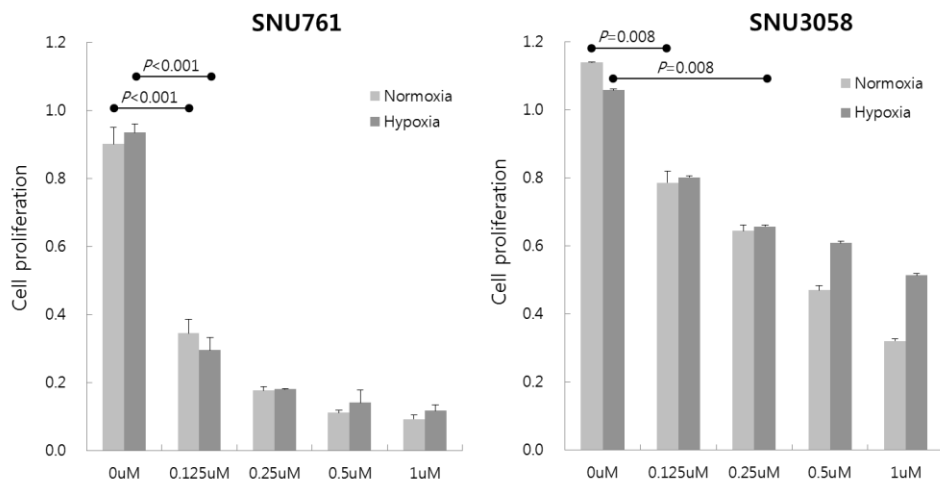

Figure 1. Anti-tumor effects of CKD-5 on SNU-761 and SNU-3085. (A) 24-hour and (B) 48-hour incubation. CKD-5 treatment significantly attenuated HCC cell proliferation in both normoxic and hypoxic conditions in a dose-dependent manner.

A

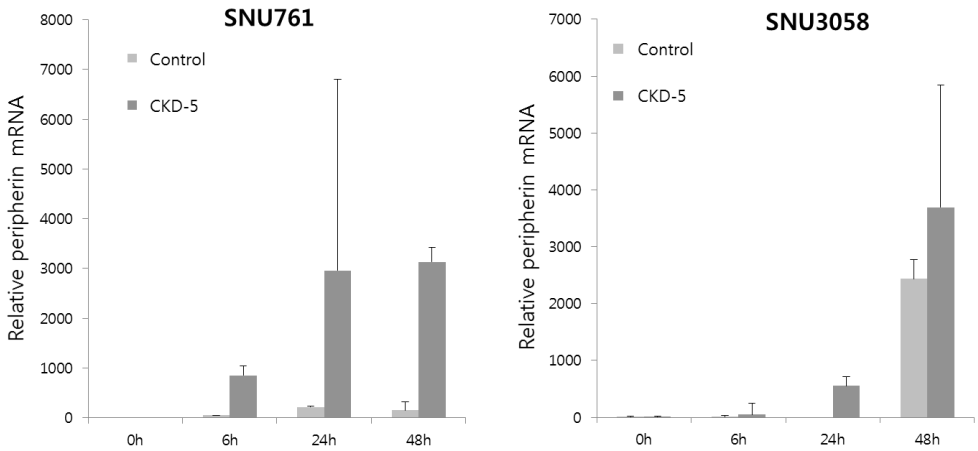
SNU761
Control
CKD-5
Relative peripherin mRNA
8000
7000
6000
5000
4000
3000
2000
1000
0
0h
6h
24h
48h
SNU3058
Control
CKD-5
Relative peripherin mRNA
7000
6000
5000
4000
3000
2000
1000
0
0h
6h
24h
48h

B

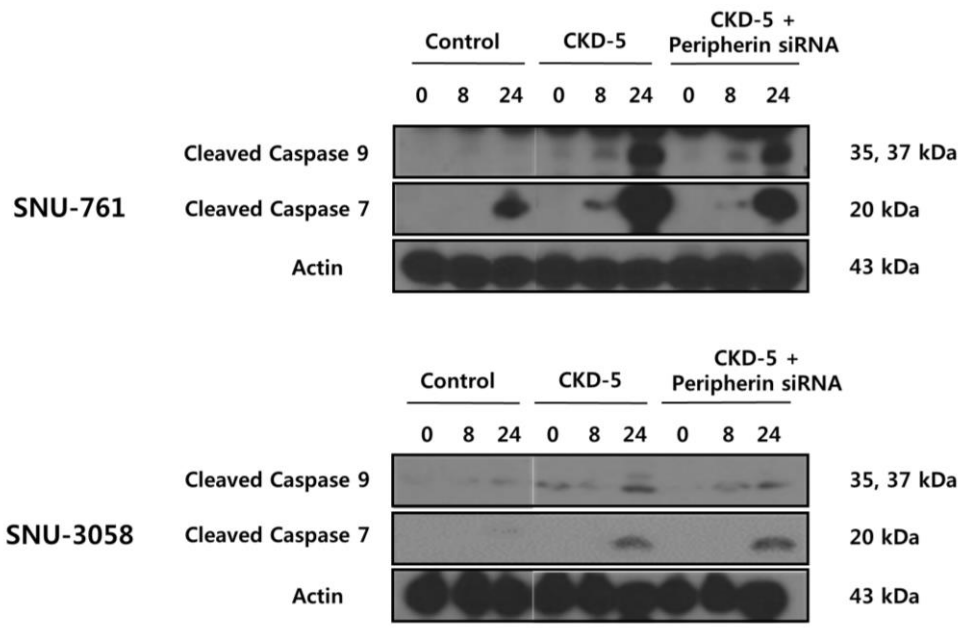
Control
CKD-5
CKD-5 +
Peripherin siRNA
0 8 24 0 8 24 0 8 24
SNU-761
Cleaved Caspase 9
Cleaved Caspase 7
Actin
35, 37 kDa
20 kDa
43 kDa
Control
CKD-5
CKD-5 +
Peripherin siRNA
0 8 24 0 8 24 0 8 24
SNU-3058
Cleaved Caspase 9
Cleaved Caspase 7
Actin
35, 37 kDa
20 kDa
43 kDa

C

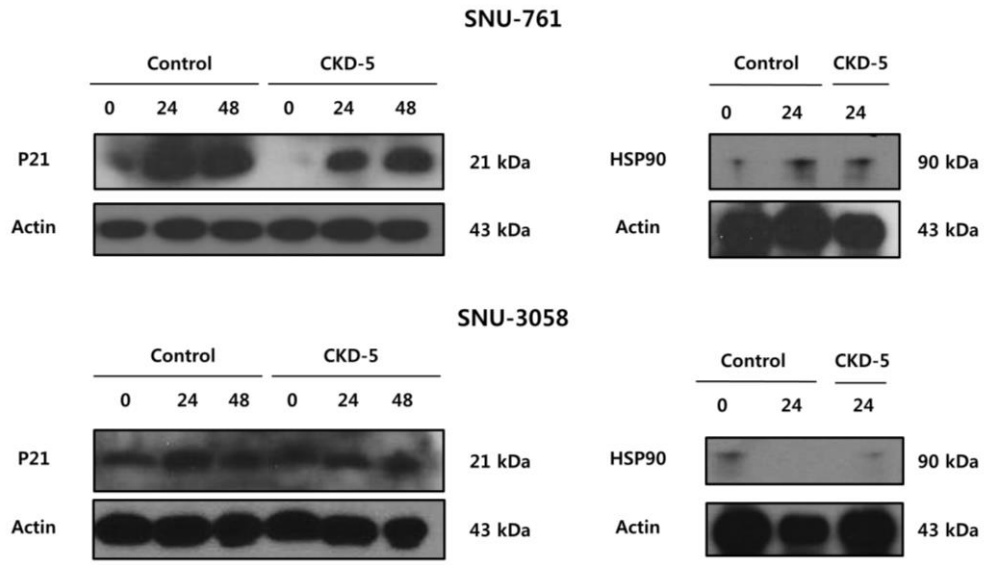

Figure 2. The mechanism of anti-tumor effects of CKD-5. (A) Peripherin mRNA was significantly overexpressed after CKD-5 treatment compared to control treatment in both SNU-761 and SNU-3058 cells. (B) CKD-5 treatment increased cleaved caspase-7 and -9 expression, which was downregulated after knockdown of peripherin with peripherin-specific siRNA in both SNU-761 and SNU-3058 cells. (C) Neither acetylated-HSP90 nor p21 expression was altered after CKD-5 treatment in both SNU-761 and SNU-3058 cells.

Data were expressed as the mean ± SD. *, $P<0.05$

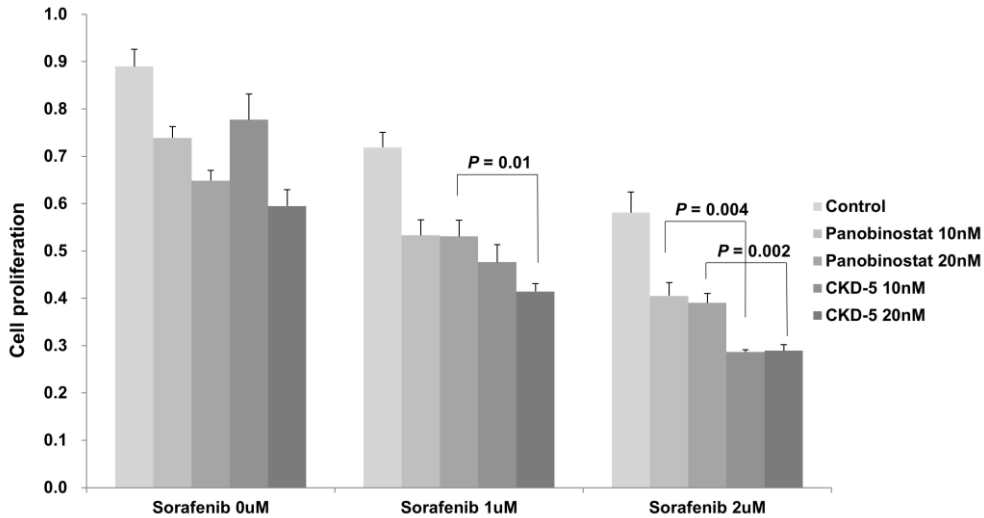

Figure 3. The cytotoxic efficacy of CKD-5 and panobinostat in SNU-761 cells. Both panobinostat and CKD-5 treatment reduced cell proliferation, and the cytotoxic efficacy was more potent in CKD-5 than panobinostat especially when combined with Sorafenib

Data were expressed as the mean ± SD. *, $P<0.05$

A

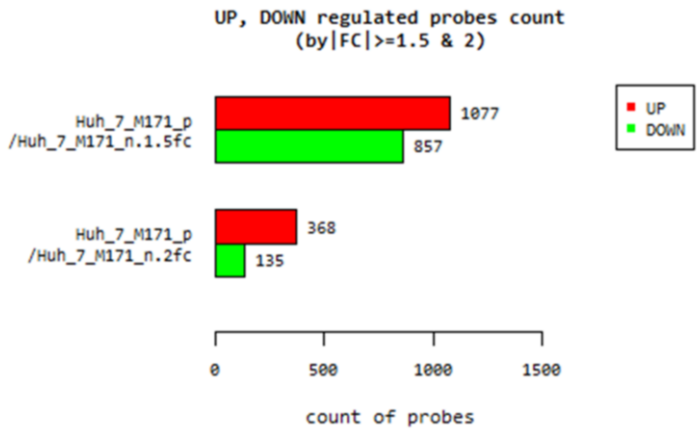
UP, DOWN regulated probes count
(by|FC|>=1.5 & 2)
Huh_7_M171_p
/Huh_7_M171_n.1.5fc
1077
857
Huh_7_M171_p
/Huh_7_M171_n.2fc
368
135
UP
DOWN
0
500
1000
1500
count of probes

B

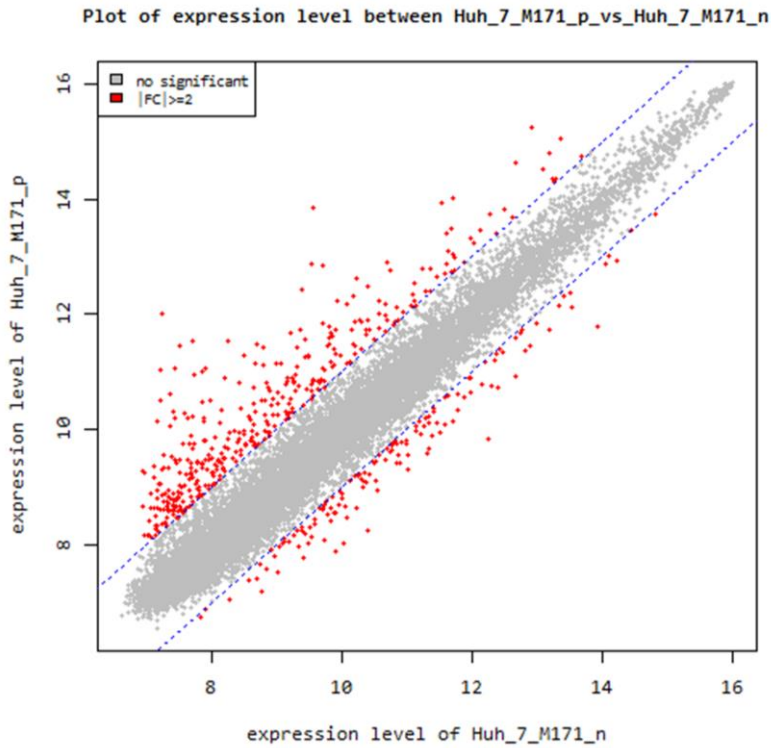
Plot of expression level between Huh_7_M171_p_vs_Huh_7_M171_n
no significant
|FC|>=2
expression level of Huh_7_M171_p
8
10
12
14
16
expression level of Huh_7_M171_n

C

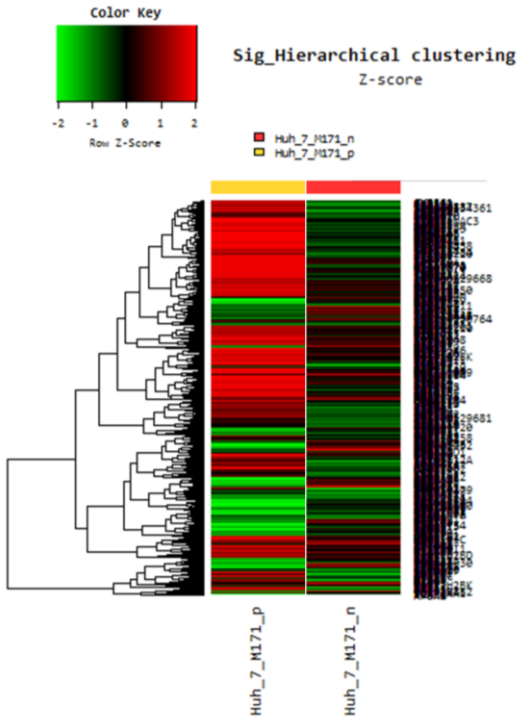

Figure 4. Results of cDNA microarray assay. (A) The number of up- or down-regulated probes filtered by P-value and various fold changes. (B) A scatter plot of expression level between the control and HDACi-treated samples. (C) Hierarchical clustering heatmap.

Data were expressed as the mean ± SD. *, $P<0.05$

A

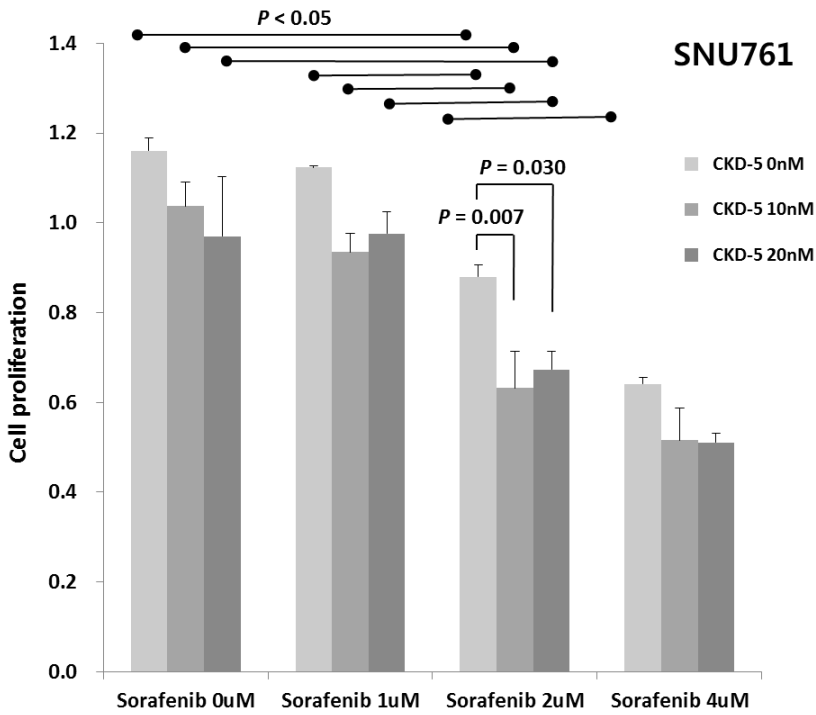
P < 0.05
SNU761
P = 0.030
P = 0.007
CKD-5 0nM
CKD-5 10nM
CKD-5 20nM
Cell proliferation
1.4
1.2
1.0
0.8
0.6
0.4
0.2
0.0
Sorafenib 0uM
Sorafenib 1uM
Sorafenib 2uM
Sorafenib 4uM

B

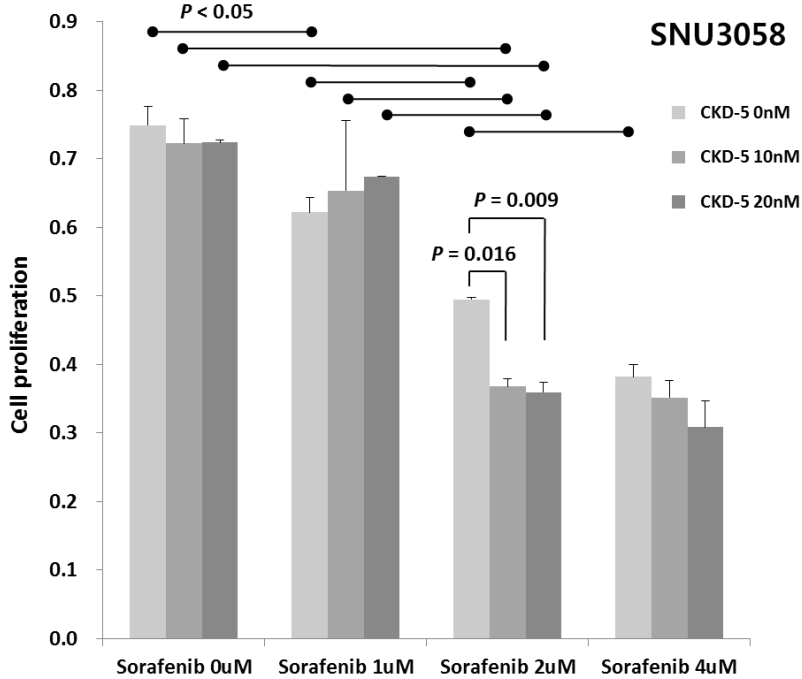
P < 0.05
SNU3058
P = 0.009
P = 0.016
CKD-5 0nM
CKD-5 10nM
CKD-5 20nM
Cell proliferation
0.9
0.8
0.7
0.6
0.5
0.4
0.3
0.2
0.1
0.0
Sorafenib 0uM
Sorafenib 1uM
Sorafenib 2uM
Sorafenib 4uM

C

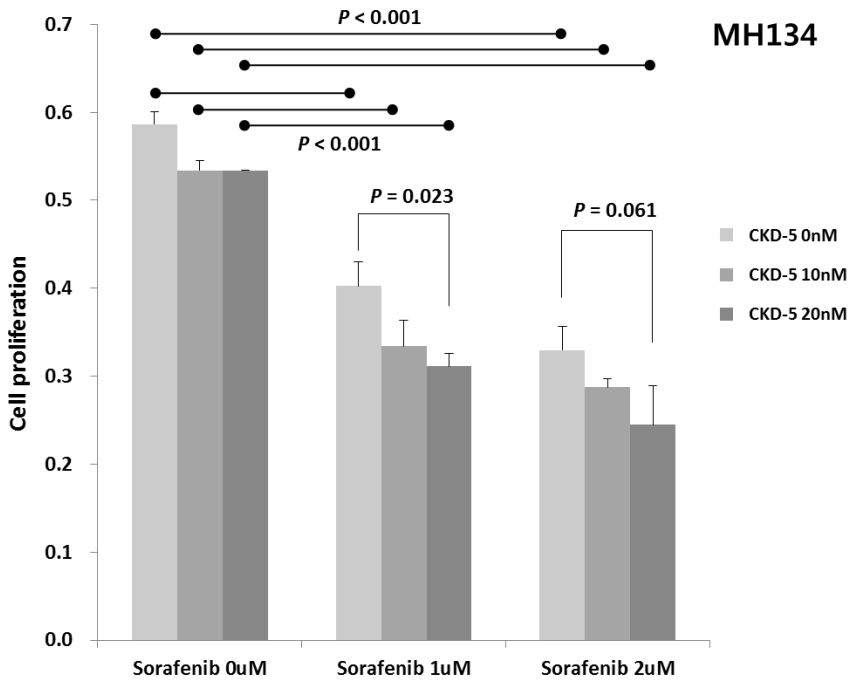
MH134
P < 0.001
P < 0.001
P = 0.023
P = 0.061
Cell proliferation
0.7
0.6
0.5
0.4
0.3
0.2
0.1
0.0
CKD-5 0nM
CKD-5 10nM
CKD-5 20nM
Sorafenib 0uM
Sorafenib 1uM
Sorafenib 2uM

D

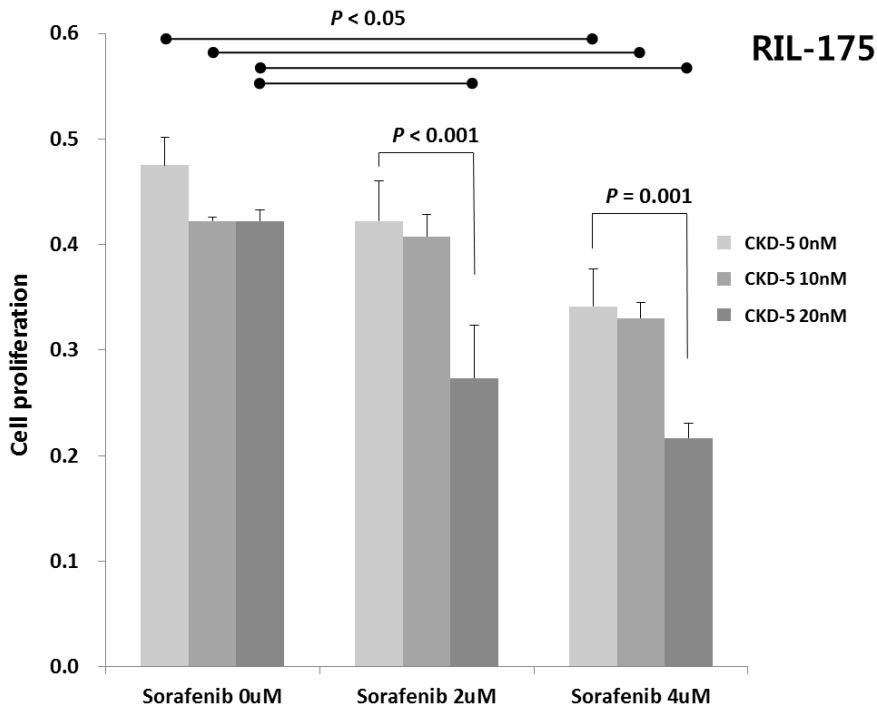
RIL-175
P < 0.05
P < 0.001
P = 0.001
Cell proliferation
0.6
0.5
0.4
0.3
0.2
0.1
0.0
CKD-5 0nM
CKD-5 10nM
CKD-5 20nM
Sorafenib 0uM
Sorafenib 2uM
Sorafenib 4uM

Figure 5. Synergistic anti-tumor effects of CKD-5 in combination with sorafenib. (A) SNU-761, (B) SNU-3058, (C) MH-134 and (D) RIL-175 cells. Combination therapy of CKD-5 with sorafenib significantly decreased HCC cell proliferation compared to CKD-5 or sorafenib monotherapy.

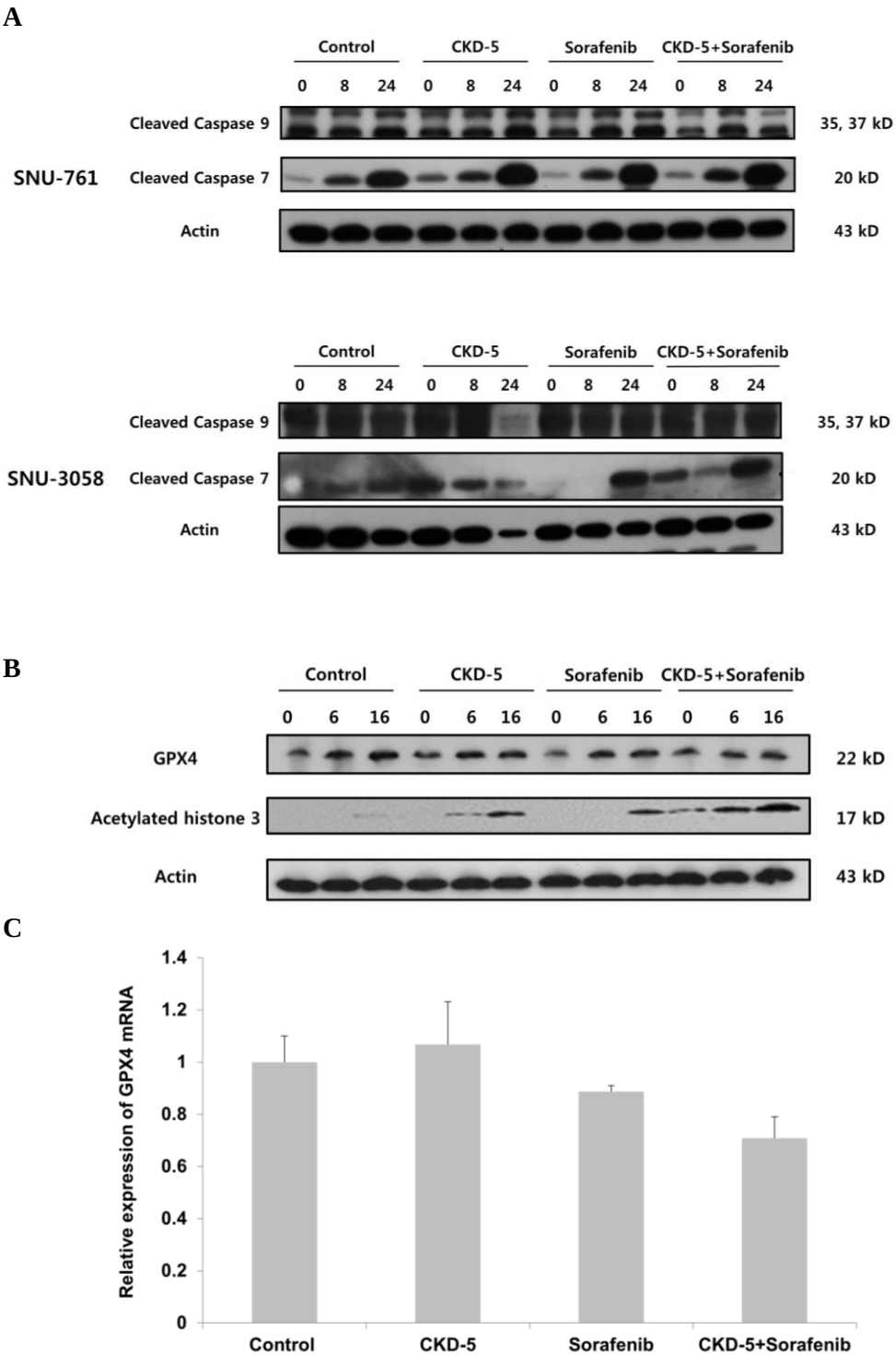
A
Control
CKD-5
Sorafenib
CKD-5+Sorafenib
0 8 24 0 8 24 0 8 24 0 8 24
Cleaved Caspase 9
35, 37 kD
SNU-761
Cleaved Caspase 7
20 kD
Actin
43 kD
Control
CKD-5
Sorafenib
CKD-5+Sorafenib
0 8 24 0 8 24 0 8 24 0 8 24
Cleaved Caspase 9
35, 37 kD
SNU-3058
Cleaved Caspase 7
20 kD
Actin
43 kD
B
Control
CKD-5
Sorafenib
CKD-5+Sorafenib
0 6 16 0 6 16 0 6 16 0 6 16
GPX4
22 kD
Acetylated histone 3
17 kD
Actin
43 kD
C
Relative expression of GPX4 mRNA
1.4
1.2
1
0.8
0.6
0.4
0.2
0
Control
CKD-5
Sorafenib
CKD-5+Sorafenib

Figure 6. The mechanism of anti-tumor effects of CKD-5 and sorafenib combination therapy. (A) Cleaved caspase-7 and -9 were highly expressed with CKD-5 and sorafenib combination therapy. (B) CKD-5 and sorafenib monotherapy increased acetylated histone H3 levels, which were further increased by the combination treatment with CKD-5 and sorafenib. GPX4 expression was reduced by sorafenib treatment, and further decreased by the combination treatment of sorafenib and CKD-5. (C) mRNA expression of GPX4 was reduced by sorafenib treatment, which was further decreased by the combination treatment of sorafenib and CKD-5.

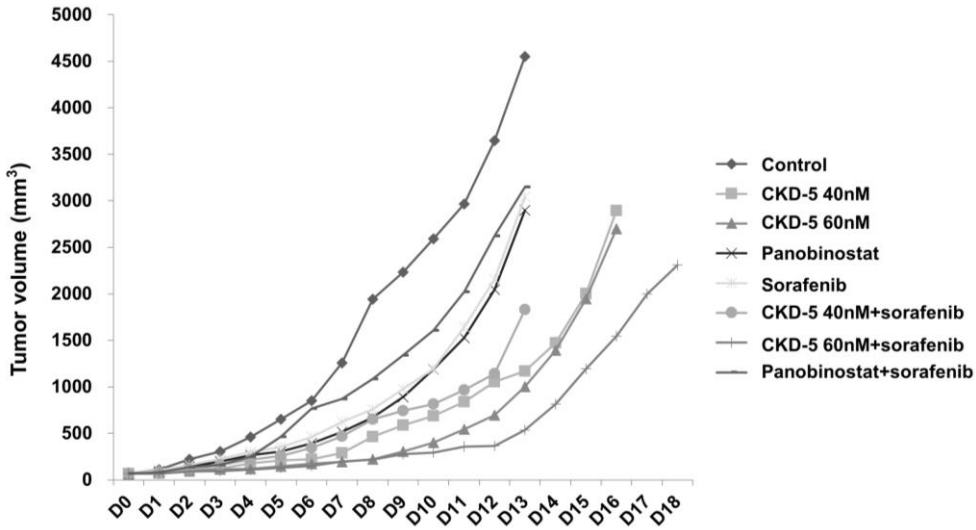

Figure 7. Changes in tumor volume over time after each treatment in a model of C3H mouse implanted with MH-134 cells. Combination therapy of high dose CKD-5 with sorafenib significantly suppressed tumor growth more than any other treatment.

A

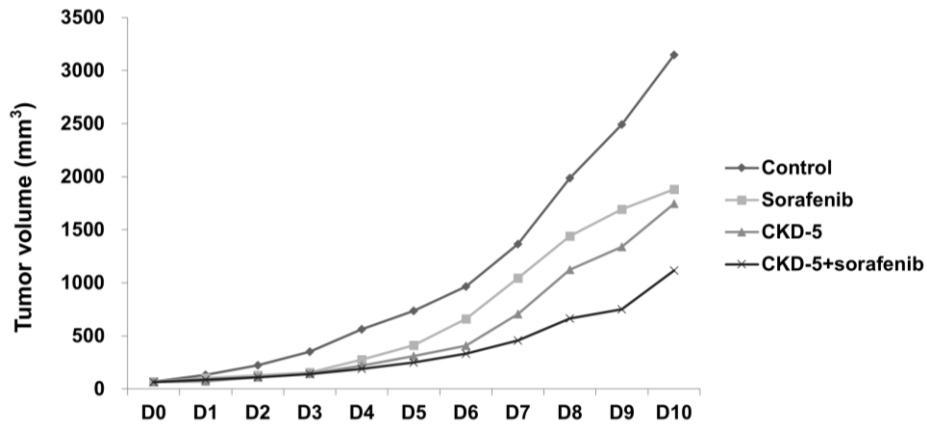
3500
3000
2500
2000
1500
1000
500
0
Tumor volume (mm3)
D0
D1
D2
D3
D4
D5
D6
D7
D8
D9
D10
Control
Sorafenib
CKD-5
CKD-5+sorafenib

B

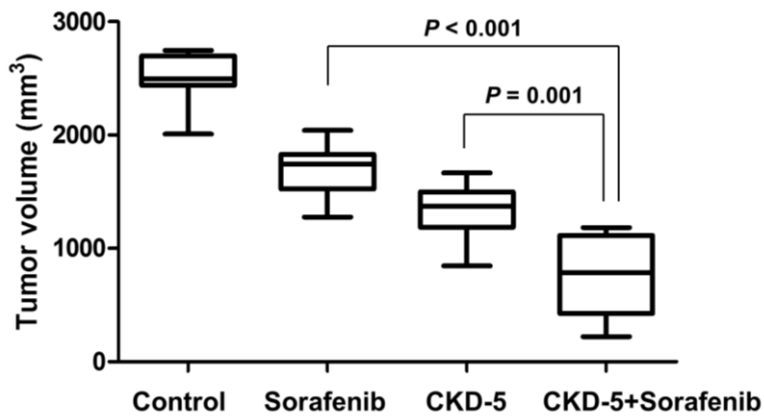
3000
2000
1000
0
Tumor volume (mm3)
P < 0.001
P = 0.001
Control
Sorafenib
CKD-5
CKD-5+Sorafenib

C

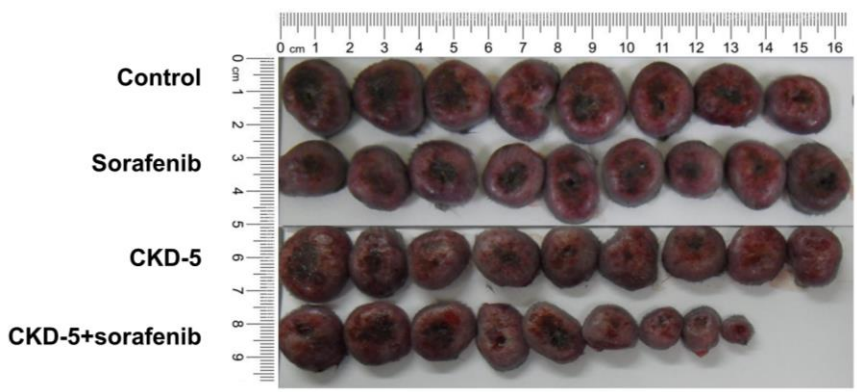
Control
Sorafenib
CKD-5
CKD-5+sorafenib

Figure 8. Results of C3H mice implanted with MH-134 cells. (A) Changes in tumor volume over time after each treatment. (B) Tumor volumes at the end of each treatment in (C) Gross specimen of tumors at the end of each treatment. Combination therapy of CKD-5 with sorafenib significantly suppressed tumor growth more than either sorafenib or CKD-5 monotherapy. The numbers of mice assigned to each treatment group are as follows: control (n = 8), sorafenib (n = 9), CKD-5 (n = 9), and CKD-5 plus sorafenib (n = 9).

.

A

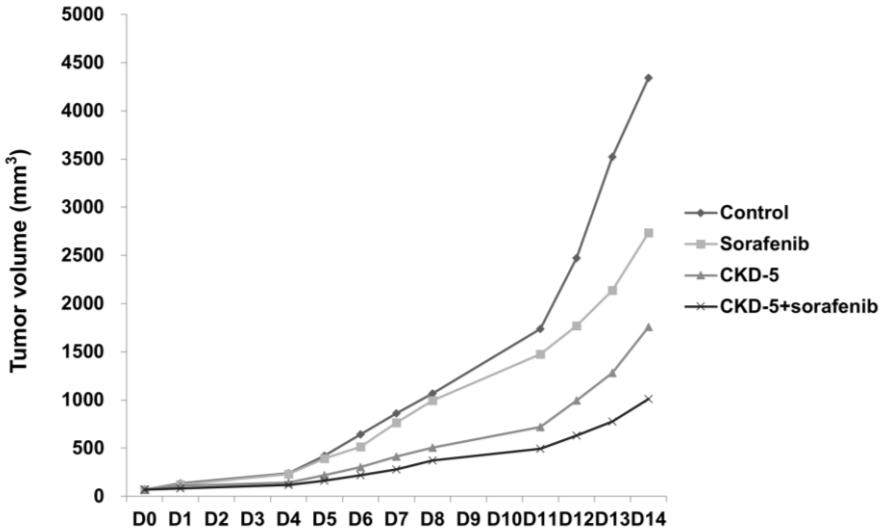
Tumor volume (mm3)
5000
4500
4000
3500
3000
2500
2000
1500
1000
500
0
D0 D1 D2 D3 D4 D5 D6 D7 D8 D9 D10 D11 D12 D13 D14
Control
Sorafenib
CKD-5
CKD-5+sorafenib

B

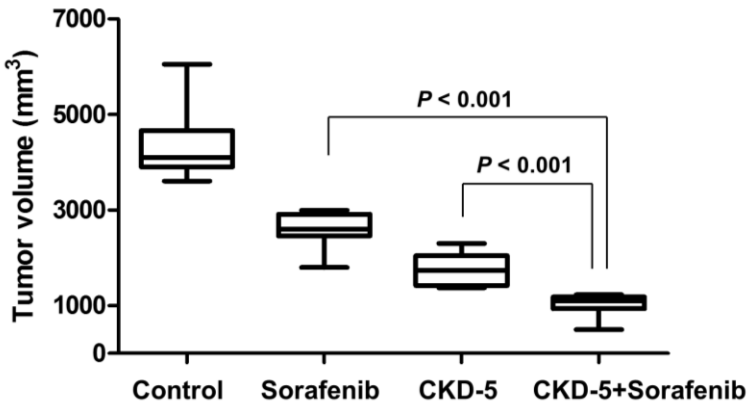
Tumor volume (mm3)
7000
5000
3000
1000
0
P < 0.001
P < 0.001
Control
Sorafenib
CKD-5
CKD-5+Sorafenib

C

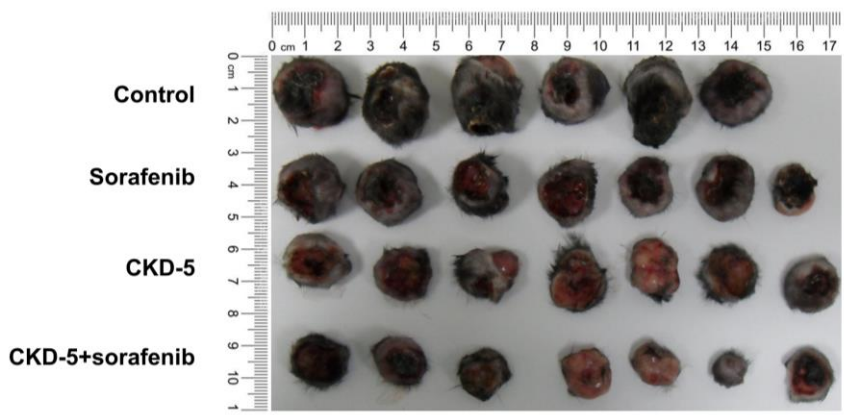
Control
Sorafenib
CKD-5
CKD-5+sorafenib

Figure 9. Results of C57BL/6 mice implanted with RIL-175 cells. (A) Changes in tumor volume over time after each treatment. (B) Tumor volumes at the end of each treatment in (C) Gross specimen of tumors at the end of each treatment. Combination therapy of CKD-5 with sorafenib significantly suppressed tumor growth more than either sorafenib or CKD-5 monotherapy. The numbers of mice assigned to each treatment group are as follows control (n = 6), sorafenib (n = 7), CKD-5 (n = 7), and CKD-5 plus sorafenib (n = 7).

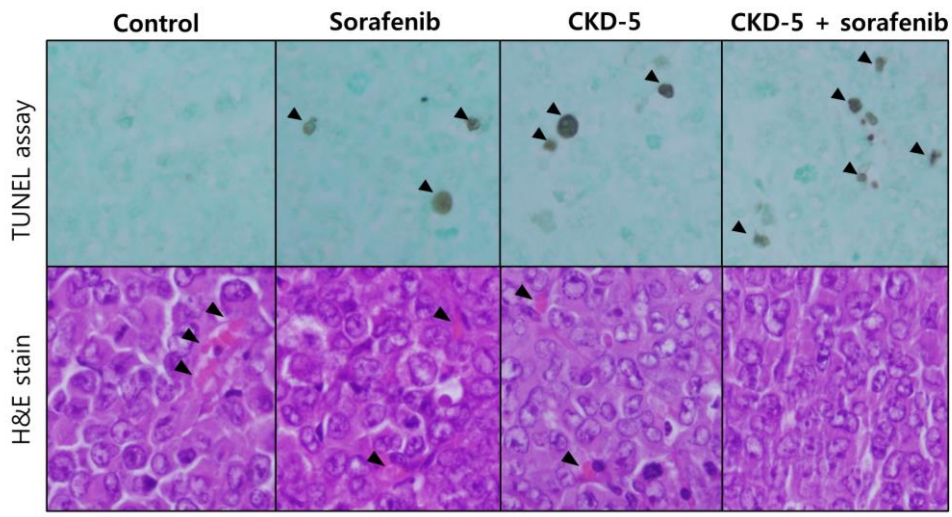

Figure 10. Apoptosis and microvessel density in tumor tissue after each treatment. Combination therapy of CKD-5 with sorafenib markedly increased apoptosis and decreased vessel density compared with CKD-5 or sorafenib monotherapy.

A

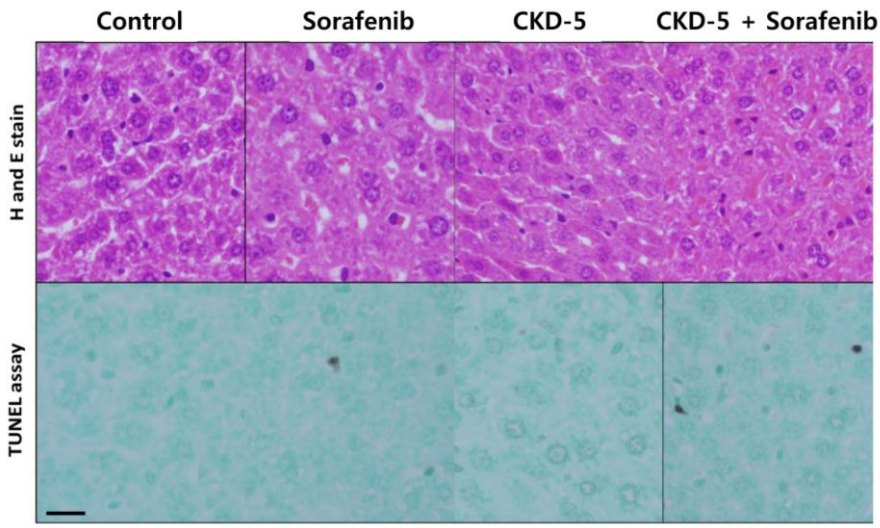

B

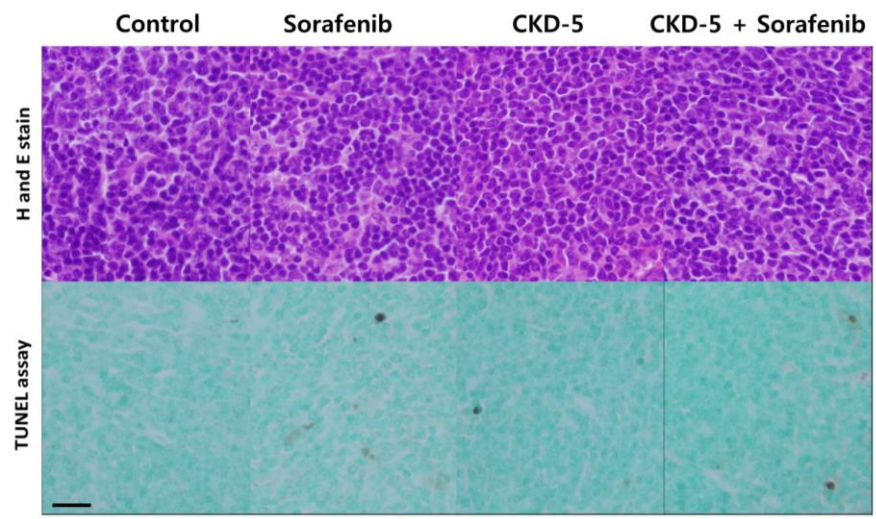

Figure 11. The degree of apoptosis in (A) liver and (B) spleen tissue. Little apoptosis of the liver and spleen tissue was detected in all treatment groups.

Tables

Table 1. A list of genes up-regulated with fold change ≥ 2 in cDNA microarray analysis

CRABP2 NPPB AIF1L PRPH PTH2 CA4 UCA1 LOC100129681 FLJ35767 CGA PGC CNFN C15orf48 IFI6 MAGEB2 SNCA GMFG COL1A2 TMEM158 ULBP2 PODXL HLA-DMB MFGE8 COL1A2 CLCNKA CLCNKA HLA-B ATP8B3 NELL2 OAS3 ARMCX2 MT1G MX1 TMSB15A PPP1R1A HAMP NDRG4 ISG15 MT2A TMEM151A IFI6 GAGE2B CD79B COL11A1 IRF9 CDC42EP5 KLRC2 UPK1A EFHD1 ELOVL4 SYT11 MUC13 VCX2 CRIP2 VCX2 SERPINE2 CT45A4 CPE KREMEN2 ACVRL1 IL8 CGB1 NPAS1 TPD52L1 NTS IL1R2 LIPG ATP6V0E2 TIMP2 KCNS1 HEY1 MAGEA9B BHMT IL13RA2 EPSTI1 COL8A2 ULBP1 CD14 PARM1 HLA-E IGFBP4 CREG1 CT45A4 VCX3A CDKN1A MT1A IL8 S100A9 PPP2R2B HLA-DRA MAGEA4 PTGER4 FXYD5 DLL3 ADAP2 VCX2 FAM125A LOC124220 PTPLA MTMR11 VCX3A PRNP INHBE GLIPR2 NLRP7 VCX2 ICAM2 FSTL3 TNFSF9 C12orf39 MT1H OLFML2A ADAM19 CCNB3 CYFIP2 SLPI CPA4 TESC LOC401720 OLR1 RGS17 SLC7A8 CENTA1 WAS CCDC151 LOC346887 CRLF1 GAD1 EDN1 C1QL4 ANKRD24 KIF5C VCX-C APLP1 SERPINI1 PLAT SERPINI1 CYR61 IFIT1 RGS22 RGS10 LIPG SMPDL3B HERC5 GPSM1 ATF3 LMTK3 DEFB1 PRNP FHL1 QPCT TIMP4 CT45A4 LOC100134361 TMEM145 IGSF11 GPR160 MSX1 KCNK6 CYP2S1 SOCS2 ROBO3 ANXA1 PCDH20 CPT1C MGC57346 PAGE1 TMEM59L CLTB GRM3 ZNF280A SAMD11 CD47 FYN DUSP1 VCX MCD1 TMEM154 MGC39900 LGMN ALPK2 FLRT2 C4orf49 HIS T1H2BK SLC1A3 FAM84B IFIH1 NRIP3 ST6GALNAC3 C11orf70 FBLN2 PRSS23 NRGN BEX5 ARL14 OC342979 C4orf49 SOX18 PRIC285 HIST1H1C APOD LUM RBP7 PRSS35 PLEK2 CD24 REEP2 CLDN11 CCDC74B HSD17B6 BIRC3 UACA MT1E MAGEB6B PI3 SAA1 CADM1 SRPX ABCB1 ELMO1 NCF2 SSX1 GJA1 NLF2 XAGE2B FAM19A2 HIST1H2BD CLDN18 LOC647784 PMP22 F2RL1 SAA2 CAND2 S100A3 LEPREL1 TNFRSF12A LOC338758 PDGFD KRT10 MTE FAM19A2 CD9 OSAP LGMN PARP9 LPHN1 FEZ1 COL8A2 PCDHB6 SMPDL3B RFTN1 XAGE1B SEMA4F MGC39900 OAS1 CFD MT1X CAV1 TPD52L1 SOCS2 MAGEH1 C1orf61 LOC653110 RNASEL HPSE BEX2 LYN HERC6 PCSK1N CER1 MT1F TMEM154 PLSCR1 MOXD1 HIST1H4H TFPI2 RASIP1 FZD9 CCNB3 CT45A5 NOS3 CPT1A NEO1 DDX60 SMAD7 MYH6 SLC2A10 RNASEL TUSC3 LIPA IRX3 F2RL1 SSX4B ENO3 S100A4 KLRC3 RABAC1 BIRC3 TRK1 LOC645558 HES4 CTSL1 NLRP2 NUAK1 GLT8D2 PLAC8 SCPEP1 CNIH2 CT45A5 NNMT LOC100129668 ITGA2 CDCP1 ACSL5

TMEM125 SCAMP5 C11orf70 LOC92249 TGFB2 TSPAN8 ONECUT2 DKK3 SYT1 OSGIN2 TAP1 LOC387882 TRIM36 NLRP7 TUBB2B TRIB1 SILV FLJ22184 FABP5L2 CAV2 CD83 TSPAN7 SMPDL3B HEG1 GOLM1 FAM108C1 SLC25A24 COL24A1 C14orf72 FABP5 SDF2L1 SEC11C IDS GEM RASL10A HIST1H2BK CYB561 CHSY1 PAGE2 CDS1 PLAC8 SLC46A3 LOC732150 PAGE2B FAM104B BHLHB2 DPYSL3 CAPRIN2 EOMES CYB561

Table 2. Growth inhibition rates of each treatment.

Cell lines	Control	CKD-5	Sorafenib	CKD-5+Sorafenib		Excess over Bliss score[†]
				Predicted[*]	Observed	
SNU-761	0.00	0.16	0.45	0.54	0.56	0.02
SNU-3058	0.00	0.03	0.49	0.51	0.59	0.08
MH-134	0.00	0.09	0.44	0.49	0.58	0.09
RIL-175	0.00	0.11	0.28	0.36	0.54	0.18

[*]Predicted cell inhibition rate which was calculated assuming drug independence according to Bliss: $M_A + M_B - M_AM_B = M_{AB}$

[†]Excess over Bliss score = $y_{ab} - \hat{y}_{ab}$

M, mortality; ŷ, predicted response; y, observed response

Table 3. Results of biochemical tests to evaluate renal and hepatic toxicity of sorafenib and CKD-5 treatment.

	Control	Sorafenib	CKD-5	CKD-5 + sorafenib
Creatinine (mg/dL)	0.4 ± 0.03	0.4 ± 0.04	0.4 ± 0.02	0.4 ± 0.04*
ALT (mg/dL)	221.5 ± 188.7	78.4 ± 45.4*	67.8 ± 42.0*	70.0 ± 30.7*
AST (mg/dL)	578.3 ± 166.2	452.7 ± 77.2	378.9 ± 154.0*	412.4 ± 91.8
Weight (g)	25.6 ± 0.9	25.0 ± 1.0	24.8 ± 1.3	24.7 ± 1.2

ALT, alanine transaminase; AST, aspartate transaminase

* $P < 0.05$ compared to control.

Discussion

Sorafenib was the first approved targeted agent in advanced HCC, achieving a significantly prolonged median survival time of 10.7 months in the treatment group compared to 7.9 months in a control group that received supportive care only.[2] However, the need for a new therapeutic agent or a combination agent with sorafenib has emerged due to the limited efficacy of sorafenib monotherapy.[3] Many clinical trials investigating effective anti-tumor agents in combination with sorafenib have failed to prove the superiority of combination therapy over sorafenib monotherapy.[37] In response to this need, we investigated the efficacy of the combination of sorafenib and CKD-5, a novel pan-HDACI that was found to have an acceptable safety profile in a phase I study involving patients with multiple myeloma.[17]

In this study, we demonstrated the anticancer effect of CKD-5 in HCC, which was synergistically enhanced by sorafenib. *In vitro*, CKD-5 monotherapy reduced cell viability and induced HCC cell apoptosis, and peripherin was involved in CKD-5-mediated HCC apoptosis. Other known HDACI-related mediators such as P21 and HSP90 were not associated with CKD-5 treatment. When combined with sorafenib, CKD-5 synergistically inhibited HCC proliferation. *In vivo*, CKD-5 alone decreased tumor volume in treated mice compared to controls, and the combination of CKD-5 and sorafenib synergistically reduced tumor volume in the mouse models. There were no demonstrable major organ toxicities. These results indicate the potential efficacy and safety of combination therapy with CKD-5 and sorafenib.

Generally, HDACIs manifest a direct anti-cancer effect by hyperacetylating histone or non-histone proteins. Several HDACIs with proven clinical efficacy for cancer treatment have received US FDA approval. Vorinostat and romidepsin for cutaneous T-cell lymphoma [38, 39], belinostat for relapsed or refractory peripheral T-cell lymphoma [40], and panobinostat for multiple myeloma [41] were sequentially approved. Although the anticancer effects of HDACIs are largely seen in hematologic malignancies, they have also been demonstrated in preclinical studies of solid cancers, particularly when administered in combination with various other treatments: with lapatinib in colon cancer [42], irradiation in non-small cell lung cancer [43], and sorafenib in HCC.[15] Further, in a recently reported case of panobinostat treatment in combination with sorafenib, a patient with advanced stage HCC showed a partial response.[44] Panobinostat, approved as a treatment in multiple myeloma, is a non-selective HDACI. We used panobinostat as a combination agent with sorafenib to compare its anticancer efficacy with CKD-5. As a result, CKD-5 showed higher anticancer efficacy than panobinostat when combined with sorafenib. This result demonstrates that anti-cancer effects of various HDACIs vary by tumor type and CKD-5 may have a greater efficacy in HCC than panobinostat.

We have identified peripherin as a possible mechanism of anticancer activity of CKD-5 by cDNA microarray analysis and it was validated with real-time PCR. Peripherin is a protein-coding gene that encodes a type III intermediate filament protein found in the neurons of the peripheral nervous system.[45] Its function and related diseases have not been fully understood, and there are only reports confined

to the nervous system, such as axonal regrowth [46] or amyptrophic lateral sclerosis.[47-49] Recently, Revill *et al*.[50] have reported peripherin as one of 13 novel tumor suppressor candidate genes in HCC, although two other genes were finally selected after subsequent validation. Enrichr analysis showed that peripherin was a negative target of the polycomb repressive complex 2 (PRC2).[51] PRC2 is one of the two classes of polycomb-group proteins, which has histone methyltransferase activity and primarily methylates histone H3.[52, 53] PRC2 is known to interact with HDACs in transcriptional silencing and is related to tumor suppressor loss.[54, 55] These studies suggest that CKD-5-induced peripherin may act as a tumor suppressor by repressing PRC2.

A recent study has reported that inhibition of HDAC is one of the anticancer activities of sorafenib, and upregulated HDAC activity may contribute to the development of sorafenib resistance.[56] In this study, we demonstrated that both CKD-5 and sorafenib increased histone acetylation, which was further enhanced with combination of CKD-5 and sorafenib. These findings suggest that CKD-5, a novel HDACi, enhanced the anticancer activity of sorafenib by amplifying the HDAC inhibitory activity of sorafenib. Several reports showed that the anticancer efficacy of sorafenib was enhanced or restored by HDAC inhibition with various agents. Statins have been reported to assist in overcoming the hypoxic resistance of HCC cells to sorafenib by inhibition of HDAC.[57] Methotrexate showed synergistic anticancer effects in combination with sorafenib through HDAC inhibition.[58] Panobinostat, the first reported HDACI, showed synergistic anticancer efficacy with

sorafenib in a preclinical study and a case report.[15, 44] In the present study, CKD-5 demonstrated superior anticancer efficacy compared to panobinostat in combination with sorafenib.

Ferroptosis is a recently recognized mechanism of regulated cell death that is distinct from apoptosis and necroptosis.[59] Glutathione peroxidase 4 (GPX4) is known as the central regulator of ferroptosis; a decrease in GPX4 expression is a signal of ferroptosis. Ferroptosis is involved in various diseases, including cancer [60], and sorafenib induces ferroptosis in HCC.[61] This was also confirmed in our study. Furthermore, we found that the induction of ferroptosis was enhanced by the combination of sorafenib with CKD-5.

There are several limitations in this study. Although the synergistic anticancer effect of combination therapy with CKD-5 and sorafenib was demonstrated using an appropriate statistical model, the synergistic efficacy was less significant *in vitro* than *in vivo*. The synergistic effects of CKD-5 and sorafenib may be achieved by modulating the tumor microenvironment as well as the cancer cells directly. Second, considering the tumor volumes of the animal tumor models used in this study, it can be inferred that both tumor models have rapidly growing tumor characteristics. Therefore, it is necessary to verify whether CKD-5 exhibits potent anticancer effects not only in tumors showing aggressive behavior but also in tumors with stable and indolent characteristics. Third, we evaluated apoptosis and ferroptosis by representative markers such as cleaved caspases and GPX4, and investigated vessel density morphologically by H&E staining instead of

immunohistochemical staining. In addition, the role of peripherin in the synergistic anticancer effect of CKD-5 and sorafenib has not been investigated in this study. Further studies using various molecular markers are needed to understand the mechanism of such synergism.

In conclusion, CKD-5 has direct anticancer effects and it has synergistic effects on HCC suppression when combined with sorafenib. Our results also suggest that CKD-5 may be superior to panobinostat in treating HCC.

References

1. Bray F, Ferlay J, Soerjomataram I, et al. Global cancer statistics 2018: GLOBOCAN estimates of incidence and mortality worldwide for 36 cancers in 185 countries. CA Cancer J Clin 2018.
2. Cheng AL, Kang YK, Chen Z, et al. Efficacy and safety of sorafenib in patients in the Asia-Pacific region with advanced hepatocellular carcinoma: a phase III randomised, double-blind, placebo-controlled trial. Lancet Oncol 2009;10:25-34.
3. Gauthier A, Ho M. Role of sorafenib in the treatment of advanced hepatocellular carcinoma: An update. Hepatol Res 2013;43:147-54.
4. Geschwind JF, Kudo M, Marrero JA, et al. TACE Treatment in Patients with Sorafenib-treated Unresectable Hepatocellular Carcinoma in Clinical Practice: Final Analysis of GIDEON. Radiology 2016;279:630-40.
5. Peng Z, Chen S, Wei M, et al. Advanced Recurrent Hepatocellular Carcinoma: Treatment with Sorafenib Alone or in Combination with Transarterial Chemoembolization and Radiofrequency Ablation. Radiology 2018;287:705-714.
6. Cosgrove DP, Reyes DK, Pawlik TM, et al. Open-Label Single-Arm Phase II Trial of Sorafenib Therapy with Drug-eluting Bead

Transarterial Chemoembolization in Patients with Unresectable Hepatocellular Carcinoma: Clinical Results. Radiology 2015;277:594-603.

7. Abou-Alfa GK, Johnson P, Knox JJ, et al. Doxorubicin plus sorafenib vs doxorubicin alone in patients with advanced hepatocellular carcinoma: a randomized trial. JAMA 2010;304:2154-60.

8. Patt Y, Rojas-Hernandez C, Fekrazad HM, et al. Phase II Trial of Sorafenib in Combination with Capecitabine in Patients with Hepatocellular Carcinoma: INST 08-20. Oncologist 2017;22:1158-e116.

9. Naqi N, Ahmad S, Murad S, et al. Efficacy and safety of sorafenib-gemcitabine combination therapy in advanced hepatocellular carcinoma: an open-label Phase II feasibility study. Hematol Oncol Stem Cell Ther 2014;7:27-31.

10. Abou-Alfa GK, Yen CJ, Hsu CH, et al. Phase Ib study of codrituzumab in combination with sorafenib in patients with non-curable advanced hepatocellular carcinoma (HCC). Cancer Chemother Pharmacol 2017;79:421-429.

11. Turcios L, Vilchez V, Acosta LF, et al. Sorafenib and FH535 in combination act synergistically on hepatocellular carcinoma by

targeting cell bioenergetics and mitochondrial function. Dig Liver Dis 2017;49:697-704.

12. Duffy AG, Ma C, Ulahannan SV, et al. Phase I and Preliminary Phase II Study of TRC105 in Combination with Sorafenib in Hepatocellular Carcinoma. Clin Cancer Res 2017;23:4633-4641.

13. Prince HM, Bishton MJ, Harrison SJ. Clinical studies of histone deacetylase inhibitors. Clin Cancer Res 2009;15:3958-69.

14. West AC, Johnstone RW. New and emerging HDAC inhibitors for cancer treatment. J Clin Invest 2014;124:30-9.

15. Lachenmayer A, Toffanin S, Cabellos L, et al. Combination therapy for hepatocellular carcinoma: additive preclinical efficacy of the HDAC inhibitor panobinostat with sorafenib. J Hepatol 2012;56:1343-50.

16. Kim SJ, Kim UJ, Yoo HY, et al. Anti-Cancer Effects of CKD-581, a Potent Histone Deacetylase Inhibitor against Diffuse Large B-Cell Lymphoma. Int J Mol Sci 2020;21.

17. Cho H, Yoon DH, Kim KP, et al. Phase I study of CKD-581, a pan-histone deacetylase inhibitor, in patients with lymphoma or multiple myeloma refractory to standard therapy. Invest New Drugs 2018;36:877-885.

18. Lee C, Ahn K-S, Jung WJ, et al. Abstract 1695: CKD-581, a novel histone deacetylase inhibitor, synergistically enhances Bortezomib cytotoxicity in multiple myeloma cells. Cancer Research 2014;74:1695-1695.

19. Kim MJ, Lee CS, Lee DH, et al. 9208 POSTER Activity of CKD-581, Histone Deacetylase Inhibitor, in Cutaneous T-cell Lymphoma Models. European Journal of Cancer 2011;47:S642.

20. Kim MJ, Lee CS, Han BH, et al. Abstract 5435: A novel HDAC inhibitor, CKD-581, demonstrates a potent in vivo efficacy in various human tumor xenograft models. Cancer Research 2010;70:5435-5435.

21. Nakabayashi H, Taketa K, Miyano K, et al. Growth of human hepatoma cells lines with differentiated functions in chemically defined medium. Cancer Res 1982;42:3858-63.

22. Lee JH, Ku JL, Park YJ, et al. Establishment and characterization of four human hepatocellular carcinoma cell lines containing hepatitis B virus DNA. World J Gastroenterol 1999;5:289-295.

23. Yoo JJ, Lee DH, Cho Y, et al. Differential sensitivity of hepatocellular carcinoma cells to suppression of hepatocystin transcription under hypoxic conditions. J Bioenerg Biomembr 2016;48:581-590.

24. Yamashita YI, Shimada M, Hasegawa H, et al. Electroporation-mediated interleukin-12 gene therapy for hepatocellular carcinoma in the mice model. Cancer Res 2001;61:1005-12.

25. Kapanadze T, Gamrekelashvili J, Ma C, et al. Regulation of accumulation and function of myeloid derived suppressor cells in different murine models of hepatocellular carcinoma. J Hepatol 2013;59:1007-13.

26. Park JG, Lee JH, Kang MS, et al. Characterization of cell lines established from human hepatocellular carcinoma. Int J Cancer 1995;62:276-82.

27. Kim KR, Moon HE, Kim KW. Hypoxia-induced angiogenesis in human hepatocellular carcinoma. J Mol Med (Berl) 2002;80:703-14.

28. Cho Y, Cho EJ, Lee JH, et al. Fucoidan-induced ID-1 suppression inhibits the in vitro and in vivo invasion of hepatocellular carcinoma cells. Biomed Pharmacother 2016;83:607-616.

29. Llovet JM, Chen Y, Wurmbach E, et al. A molecular signature to discriminate dysplastic nodules from early hepatocellular carcinoma in HCV cirrhosis. Gastroenterology 2006;131:1758-67.

30. Saijo H, Tatsumi N, Arihiro S, et al. Microangiopathy triggers, and inducible nitric oxide synthase exacerbates dextran sulfate sodium-

induced colitis. Lab Invest 2015;95:728-48.

31. Clarke WT, Edwards B, McCullagh KJ, et al. Syncoilin modulates peripherin filament networks and is necessary for large-calibre motor neurons. J Cell Sci 2010;123:2543-52.

32. Li X, Duan L, Yuan S, et al. Ferroptosis inhibitor alleviates Radiation-induced lung fibrosis (RILF) via down-regulation of TGF-beta1. J Inflamm (Lond) 2019;16:11.

33. Nakatani S, Iwagaki H, Okabayashi T, et al. Effects of streptococcal preparation OK-432 on cytokine induction in spleen and tumour tissues of mice bearing MH-134 tumour cells. J Int Med Res 1999;27:27-37.

34. Orci LA, Lacotte S, Delaune V, et al. Effects of the gut-liver axis on ischaemia-mediated hepatocellular carcinoma recurrence in the mouse liver. J Hepatol 2018;68:978-985.

35. Hou H, Lariviere JP, Demidenko E, et al. Repeated tumor pO(2) measurements by multi-site EPR oximetry as a prognostic marker for enhanced therapeutic efficacy of fractionated radiotherapy. Radiother Oncol 2009;91:126-31.

36. Liu Q, Yin X, Languino LR, et al. Evaluation of drug combination effect using a Bliss independence dose-response surface model. Stat

Biopharm Res 2018;10:112-122.

37. Kudo M. Systemic Therapy for Hepatocellular Carcinoma: 2017 Update. Oncology 2017;93 Suppl 1:135-146.

38. Olsen EA, Kim YH, Kuzel TM, et al. Phase IIb multicenter trial of vorinostat in patients with persistent, progressive, or treatment refractory cutaneous T-cell lymphoma. J Clin Oncol 2007;25:3109-15.

39. Whittaker SJ, Demierre MF, Kim EJ, et al. Final results from a multicenter, international, pivotal study of romidepsin in refractory cutaneous T-cell lymphoma. J Clin Oncol 2010;28:4485-91.

40. Lee HZ, Kwitkowski VE, Del Valle PL, et al. FDA Approval: Belinostat for the Treatment of Patients with Relapsed or Refractory Peripheral T-cell Lymphoma. Clin Cancer Res 2015;21:2666-70.

41. Laubach JP, Moreau P, San-Miguel JF, et al. Panobinostat for the Treatment of Multiple Myeloma. Clin Cancer Res 2015;21:4767-73.

42. LaBonte MJ, Wilson PM, Fazzone W, et al. The dual EGFR/HER2 inhibitor lapatinib synergistically enhances the antitumor activity of the histone deacetylase inhibitor panobinostat in colorectal cancer models. Cancer Res 2011;71:3635-48.

43. Geng L, Cuneo KC, Fu A, et al. Histone deacetylase (HDAC) inhibitor LBH589 increases duration of gamma-H2AX foci and

confines HDAC4 to the cytoplasm in irradiated non-small cell lung cancer. Cancer Res 2006;66:11298-304.

44. Knieling F, Waldner MJ, Goertz RS, et al. Quantification of dynamic contrast-enhanced ultrasound in HCC: prediction of response to a new combination therapy of sorafenib and panobinostat in advanced hepatocellular carcinoma. BMJ Case Rep 2012;2012.

45. Portier MM, de Nechaud B, Gros F. Peripherin, a new member of the intermediate filament protein family. Dev Neurosci 1983;6:335-44.

46. Oblinger MM, Wong J, Parysek LM. Axotomy-induced changes in the expression of a type III neuronal intermediate filament gene. J Neurosci 1989;9:3766-75.

47. He CZ, Hays AP. Expression of peripherin in ubiquinated inclusions of amyotrophic lateral sclerosis. J Neurol Sci 2004;217:47-54.

48. Gros-Louis F, Lariviere R, Gowing G, et al. A frameshift deletion in peripherin gene associated with amyotrophic lateral sclerosis. J Biol Chem 2004;279:45951-6.

49. Leung CL, He CZ, Kaufmann P, et al. A pathogenic peripherin gene mutation in a patient with amyotrophic lateral sclerosis. Brain Pathol 2004;14:290-6.

50. Revill K, Wang T, Lachenmayer A, et al. Genome-wide methylation

analysis and epigenetic unmasking identify tumor suppressor genes in hepatocellular carcinoma. Gastroenterology 2013;145:1424-35 e1-25.

51. Chen EY, Tan CM, Kou Y, et al. Enrichr: interactive and collaborative HTML5 gene list enrichment analysis tool. BMC Bioinformatics 2013;14:128.

52. Chase A, Cross NC. Aberrations of EZH2 in cancer. Clin Cancer Res 2011;17:2613-8.

53. Yoo KH, Hennighausen L. EZH2 methyltransferase and H3K27 methylation in breast cancer. Int J Biol Sci 2012;8:59-65.

54. Kuzmichev A, Nishioka K, Erdjument-Bromage H, et al. Histone methyltransferase activity associated with a human multiprotein complex containing the Enhancer of Zeste protein. Genes Dev 2002;16:2893-905.

55. van der Vlag J, Otte AP. Transcriptional repression mediated by the human polycomb-group protein EED involves histone deacetylation. Nat Genet 1999;23:474-8.

56. Liu TP, Hong YH, Yang PM. In silico and in vitro identification of inhibitory activities of sorafenib on histone deacetylases in hepatocellular carcinoma cells. Oncotarget 2017;8:86168-86180.

57. Zhou TY, Zhuang LH, Hu Y, et al. Inactivation of hypoxia-induced

YAP by statins overcomes hypoxic resistance tosorafenib in hepatocellular carcinoma cells. Sci Rep 2016;6:30483.

58. Lee D, Xu IM, Chiu DK, et al. Folate cycle enzyme MTHFD1L confers metabolic advantages in hepatocellular carcinoma. J Clin Invest 2017;127:1856-1872.

59. Dixon SJ, Lemberg KM, Lamprecht MR, et al. Ferroptosis: an iron-dependent form of nonapoptotic cell death. Cell 2012;149:1060-72.

60. Masaldan S, Bush AI, Devos D, et al. Striking while the iron is hot: Iron metabolism and ferroptosis in neurodegeneration. Free Radic Biol Med 2019;133:221-233.

61. Lachaier E, Louandre C, Godin C, et al. Sorafenib induces ferroptosis in human cancer cell lines originating from different solid tumors. Anticancer Res 2014;34:6417-22.

국문초록

서론: 히스톤 디아세틸라제 억제제(HDACI)는 간세포암을 비롯한 여러 암의 발생 및 약물저항성을 억제하는 역할을 하는 것으로 알려져 있다. 최근 소라페닙 내성 간세포암 환자를 대상으로 한 Ⅰ/Ⅱ상 연구에서 HDACI의 약물감작제로서의 가능성이 보고된 바 있다. 본 연구에서는 간세포암에서 새롭게 개발된 HDACI인 CKD-5와 소라페닙 병용 요법의 항암효과에 대해 분석하고자 하였다.

방법: 사람과 동물 간암세포주(SNU-761, SNU-3058, MH-134, RIL-175)에서 CKD-5 단독 및 소라페닙 병용요법의 항암 효과를 MTS 분석을 사용하여 평가하였다. 세포사멸의 기전을 분석하기 위해 microarray를 시행하였고, small interfering RNA(siRNA)감염과 웨스턴블롯 기법을 활용하여 입증하였다. 동물실험은 두 가지 다른 종류의 간세포암 마우스 모델을 사용하여 수행하였다. MH-134 세포가 이식 된 C3H 마우스와 RIL-175 세포가 이식 된 C57BL/6 마우스는 대조군, 소라페닙, CKD-5, 소라페닙과 CKD-5 병용투여군으로 나누어 2주간 투약 후 종양의 변화를 확인하였다.

결과: CKD-5는 정상 산소 상태와 저산소 상태 모두에서 사람 간암세포주의 증식을 유의하게 억제했다. 세포 사멸기전을 분석한 결과 CKD-5는 간암세포에서 peripherin 발현을 유의하게 증가 시키는 것이 확인되었고, siRNA를 통해 peripherin 발현을 억제 시 CKD-5 유도 간암세포 사멸을 감소시키는 것이 확인되었다. CKD-5와 소라페닙의 병용요법은 사람 및 동물 간암세포주 모두에서 소라페닙 또는 CKD-5 단일 요법과 비교하여 세포 증식을 더욱 효과적으로 억제

하였다. CKD-5와 소라페닙 병용요법의 효과는 두 종류의 간세포암 마우스모델에서도 일관되게 입증되었다.

결론: CKD-5는 간세포암에서 소라페닙의 항암효과를 향상시킬 수 있으며, CKD-5와 소라페닙의 병용투여는 간세포암의 새로운 치료 전략이 될 수 있다.

주요어: 히스톤 디아세틸라제 억제제; CKD-5; 간세포암; 소라페닙